

KRAB domain of ZFP568 disrupts TRIM28-mediated abnormal interactions in cancer cells

Janani Kumar¹, Gundeep Kaur¹, Ren Ren¹, Yue Lu¹, Kevin Lin¹, Jia Li², Yun Huang^{1,2}, Anamika Patel³, Michelle C. Barton¹, Todd Macfarlan⁴, Xing Zhang^{1,*} and Xiaodong Cheng^{1,*}

¹Department of Epigenetics and Molecular Carcinogenesis, University of Texas MD Anderson Cancer Center, Houston, TX 77030, USA, ²Center for Epigenetics & Disease Prevention, Institute of Biosciences and Technology, Texas A&M University, Houston, TX 77030, USA, ³Department of Biochemistry, Emory University School of Medicine, Atlanta, GA 30329, USA and ⁴The Eunice Kennedy Shriver National Institute of Child Health and Human Development, NIH, Bethesda, MD 20892, USA

Received March 15, 2020; Revised April 25, 2020; Editorial Decision April 29, 2020; Accepted April 30, 2020

ABSTRACT

Interactions of KRAB (Krüppel-associated box)-associated protein KAP1 [also known as TRIM28 (tripartite motif containing protein 28)] with DNA-binding KRAB zinc finger (KRAB-ZF) proteins silence many transposable elements during embryogenesis. However, in some cancers, TRIM28 is up-regulated and interacts with different partners, many of which are transcription regulators such as EZH2 in MCF7 cells, to form abnormal repressive or activating complexes that lead to misregulation of genes. We ask whether a KRAB domain—the TRIM28 interaction domain present in native binding partners of TRIM28 that mediate repression of transposable elements—could be used as a tool molecule to disrupt aberrant TRIM28 complexes. Expression of KRAB domain containing fragments from a KRAB-ZF protein (ZFP568) in MCF7 cells, without the DNA-binding zinc fingers, inhibited TRIM28–EZH2 interactions and caused degradation of both TRIM28 and EZH2 proteins as well as other components of the EZH2-associated polycomb repressor 2 complex. In consequence, the product of EZH2 enzymatic activity, trimethylation of histone H3 lysine 27 level, was significantly reduced. The expression of a synthetic KRAB domain significantly inhibits the growth of breast cancer cells (MCF7) but has no effect on normal (immortalized) human mammary epithelial cells (MCF10a). Further, we found that TRIM28 is a positive regulator of TRIM24 protein levels, as observed previously in prostate cancer cells, and expression of

the KRAB domain also lowered TRIM24 protein. Importantly, reduction of TRIM24 levels, by treatment with either the KRAB domain or a small-molecule degrader targeted to TRIM24, is accompanied by an elevated level of tumor suppressor p53. Taken together, this study reveals a novel mechanism for a TRIM28-associated protein stability network and establishes TRIM28 as a potential therapeutic target in cancers where TRIM28 is elevated. Finally, we discuss a potential mechanism of KRAB-ZF gene expression controlled by a regulatory feedback loop of TRIM28–KRAB.

INTRODUCTION

The family of Krüppel-associated box (KRAB) domain containing zinc finger (ZF) transcriptional regulators has expanded greatly during vertebrate evolution (1–3), largely in response to a need to repress transposable elements (4,5). Transposable elements make up a large fraction of the genome and are mostly considered genetic threats in need of the strictest silencing during embryogenesis and differentiation. However, a few recently characterized KRAB-ZF proteins are involved in determining meiotic recombination hotspots [PRDM9 (6)] and controlling allele-specific expression of imprinted genes [ZFP57 and ZFP568 (7,8)]. The KRAB-ZF proteins are generally organized into the N-terminal portion containing at least one KRAB domain and a C-terminal array of tandem ZFs (9), ranging from 3 to ~35 fingers with an average array size of 11–13 fingers (10), that can potentially bind to long stretch of DNA with sequence specificity.

The KRAB domain, a conserved ~75-residue polypeptide (11), is well characterized as an interacting part-

*To whom correspondence should be addressed. Email: xcheng5@mdanderson.org
Correspondence may also be addressed to Xing Zhang. Email: xzhang21@mdanderson.org

ner of KRAB-associated protein (KAP1) (12), a corepressor also known as tripartite motif containing protein 28 (TRIM28) (13). The interaction with a KRAB domain recruits KAP1/TRIM28 (11,14) and assembles a KAP1-associated heterochromatin complex in specific regions of chromatin, including many well-known cofactors involved in heterochromatin formation: histone H3 lysine 9 (H3K9) methyltransferase SETDB1 (15), heterochromatin protein 1 (16), histone deacetylase containing nucleosome remodeling complex (17) and DNA methyltransferases (18).

TRIM28, a large multi-domain protein, contains a distinctive N-terminal RBCC domain—a composite of RING, tandem B-box (B1 and B2) and long coiled-coil domain—and a C-terminal PHD bromodomain (19–21) (Figure 1A). This architectural organization enables TRIM28 to assemble protein cofactors in a modular fashion; i.e. TRIM28 acts as a scaffold for recruiting specific cellular machinery to target genomic locations. TRIM28 is now known to participate in many aspects of cellular biology, with many different activities. These include critical roles in early embryonic development (22) while not essential in adult mice (23), promoting proliferation and metastasis of many tumor types (24–27) and as a tumor suppressor in the formation of childhood Wilms tumor (28,29). However, the multitude and complexity of TRIM28 actions in cancer make it difficult to unambiguously establish a mechanism for TRIM28, probably because in each case TRIM28 was reported to interact with different partners, many of which are transcription regulator(s), such as transcription factors (30–32), histone methyltransferase EZH2 (33) and TRIM24 (a related member of TRIM family) (24). Interestingly, TRIM28 targets tumor suppressor protein p53 for degradation in association with other proteins, particularly ubiquitin E3 ligases MDM2 (34,35) and TRIM24 (36,37), and a melanoma antigen family member MAGE-C2 (38–40).

We hypothesize that tumor-associated TRIM28 is hijacked by other protein(s) to form irregular (abnormal) repressive or activating complexes that lead to misregulation. We ask whether a KRAB domain—the native binding partner of TRIM28 required for repression of transposable elements by KRAB-ZF proteins—could be used as a tool molecule to disrupt such aberrant TRIM28 complexes. As a proof of the concept, we use the KRAB-containing N-terminal fragment of ZFP568—a highly conserved mammalian KRAB-ZF protein that represses a transcript of placental-specific insulin-like growth factor 2 in mice (8,41)—and test the concept in breast cancer derived, estrogen receptor positive MCF7 cells where an abnormal interaction between TRIM28 and EZH2 promotes mammosphere formation (33). We observed changes in protein levels of EZH2, TRIM24, p53 and a substantial number of KRAB-ZF proteins in MCF7 cells upon introducing a peptide fragment containing the KRAB domain.

MATERIALS AND METHODS

The plasmids used for expression in *Escherichia coli* are listed in Supplementary Figure S1A and examples of purified proteins used for biophysical analyses are shown in Supplementary Figure S1B. Experimental details of multi-angle

light scattering, small-angle X-ray scattering and analytical ultracentrifugation are provided in the ‘Materials and Methods’ section in the Supplementary Data, which also includes reverse-phase protein array analysis and RNA-seq analysis.

Cell lines

MCF7, MCF10a, HEK293T and MDA-MB231 cells were cultured at 37°C under 5% CO₂. Dulbecco’s modified Eagle’s medium (DMEM)/F-12 media (Thermo Fisher) was used for MCF7 and MDA-MB231; DMEM media for HEK293T containing 10% fetal bovine serum (FBS; Atlanta Biologicals), 1% L-glutamine, 1% Pen–Strep; and MEBM containing bullet kit (Lonza) for MCF10a cells. The cells were routinely tested for mycoplasma using Lonza mycoplasma kit using manufacturer’s instructions.

Lentiviral transfection and establishment of stable cell lines

K2 fragment (residues 1–360) or K1 fragment (residues 1–105) from mouse ZFP568 was cloned onto pLJM1-eGFP lentiviral construct (Addgene plasmid #19319). KRAB lentiviral plasmid was co-transfected with packaging plasmids pPAX2 (Addgene plasmid #12260) and pMD.2G (Addgene plasmid #12259) into HEK293T cells to generate virus. After 48 h, the supernatant was collected, filtered and transferred onto targeted cell lines for infection for 48 h, followed by selection with 2 µg/ml puromycin and growth of stable resistant clones.

TRIM28 knockdown was achieved using stable pGIPZ short-hairpin interfering RNA in lentivirus (clones of shTRIM28, Clone #1: V3LHS.358497, GE Dharmacon, Lafayette, CO, USA). A lentiviral scrambled pGIPZ plasmid (GE Dharmacon) was used as control for transfection and virus packaging. Expressions of EZH2 and GAPDH were achieved using LentiORF EZH2 without stop codon (CloneId PLOHS.1000086) and LentiORF GAPDH without stop codon (CloneId PLOHS.100009204).

Growth assay

Cell growth rates in the presence and absence of KRAB domain were assessed as described (42). Briefly, 1×10^5 cells per well were seeded onto a six-well plate. Cells were trypsinized and resuspended in medium for counting using a hemocytometer daily over a 7-day period. Each experiment was performed in triplicate.

Proliferation assay

Cell proliferation was assessed using CellTiter-Glo (Promega, USA) as per manufacturer’s instructions. Briefly, ~1000 cells were seeded onto a 96-well plate. Growth of the cells was measured for a period of 7 days where the cells were trypsinized and resuspended in lysis buffer and luminescence was measured. Each experiment was performed in triplicate for each harvest and repeated thrice.

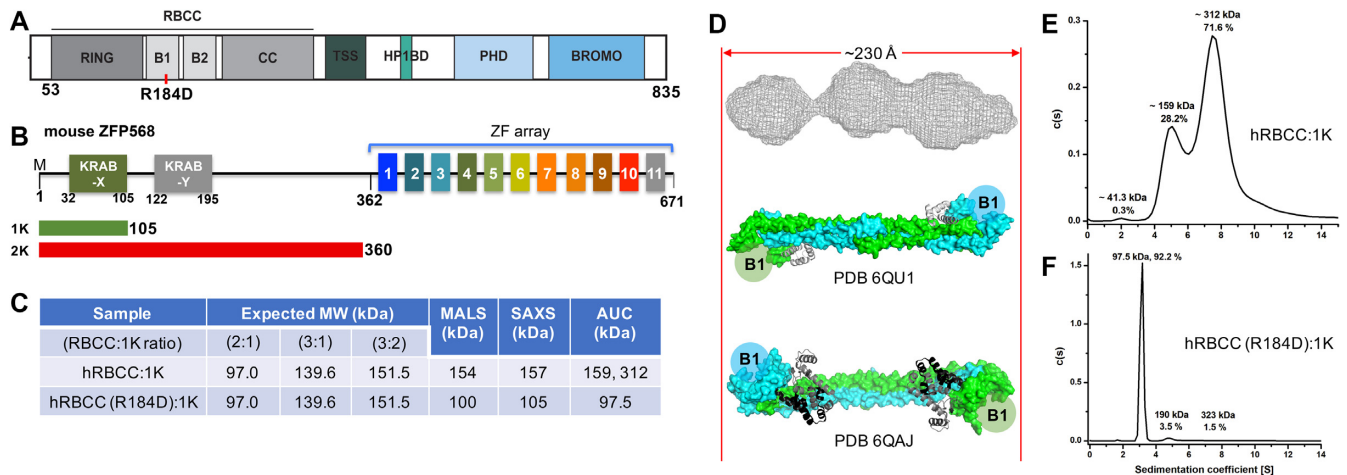


Figure 1. KRAB interaction with TRIM28. (A, B) Schematic representation of human TRIM28 and mouse ZFP568 and two KRAB-containing fragments (1K and 2K) used for expression. (C) Summary of mass measurements of hRBCC-1K complex by three biophysical methods. (D) The SAXS envelope of hRBCC-1K complex (top panel). X-ray structure of RBCC (with a deletion of B1 box) in complex with SMARCAD1 CUE1,2 (PDB 6QU1), where the CUE1 domain is in gray ribbon and CUE2 domain was not observed (middle panel) (20). X-ray structure of RBCC with an N-terminal fusion of T4 lysozyme in dark ribbon (PDB 6QAJ) (bottom panel) (19). The B1 box (as indicated) is either deleted or disordered in both structures. Sedimentation coefficient distribution profiles of hRBCC-1K complex (E) and the mutant R184D-1K complex (F).

Crystal violet staining

Cells were incubated with 2 ml of cell medium and incubated for 10 days until colonies were visible. After brief washing with phosphate-buffered saline (PBS), colonies were fixed with fixation solution (10% methanol, 10% acetic acid, 80% H₂O) for 10 min and stained with 0.4% crystal violet (200 ml of 4% crystal violet, 200 ml of H₂O and 100 ml of ethanol). Colonies containing > 50 cells were counted. The ratio of intensity was calculated using ImageJ CFU plugin.

Flow cytometry

Confluent cells were harvested for fluorescence-activated cell sorter (FACS) analysis. Cell monolayers were washed twice with PBS, detached with 0.25% (w/v) trypsin-EDTA solution, collected by centrifugation and washed additional two times with PBS. Cell cycle analysis was performed on fixed cells using propidium iodide and apoptosis was separately quantified with Annexin V-FITC using an apoptosis detection kit (BD Biosciences). In each case, samples were analyzed on a FACS Canto (BD Biosciences) using FACS DIVA software, in comparison to appropriate controls.

Migration assay

Migration assays were performed using a two-chamber Transwell, as described (43), using a polycarbonate filter with 8 μm pores. Cells were trypsinized and suspended in medium containing 0.1% (v/v) FBS at a concentration of 1 × 10⁵ cells per well. The cells were placed in the upper chamber and the medium containing 0.1% (v/v) was placed in the lower chamber. After 24 h at 37°C, the cells in the upper chamber were wiped off with a cotton swab. The cells on the lower surface of the filter were fixed with 4% (w/v) paraformaldehyde for 1 min at room temperature, permeabilized with 100% (v/v) methanol, washed with PBS and

stained with crystal violet (Sigma-Aldrich). Migration was quantitated by selecting 10 different views and the number of migrated cells was calculated.

Immunoprecipitation

Nuclear extracts were prepared as described (44). A 5 μg of the indicated antibody (Supplementary Table S1) was added to 500 μg of nuclear extracts pre-cleared with protein AG combined magnetic beads and incubated overnight at 4°C. Antibody-bound proteins were pulled down with 50 μl of protein AG combined magnetic beads and washed thrice with wash buffer containing 0.1% Triton X-100. The washed beads were resuspended in 20 μl sample buffer and used for western blot analysis.

Western blot analysis

Proteins were extracted using RIPA buffer containing complete protease inhibitors (Sigma-Aldrich) according to the manufacturer's instructions. The concentration of the protein was estimated using a Pierce BCA protein determination kit (Thermo Scientific, USA) following the manufacturer's instructions, with bovine serum albumin used as standard, and the absorbance at 562 nm determined using a multilabel plate reader. Western blot was performed as described (45), using the indicated antibodies (Supplementary Table S1).

RESULTS

ZFP568 KRAB domain interacts with TRIM28 *in vitro*

ZFP568 is unique among the members of the KRAB-ZF family, as it possesses two N-terminal KRAB domains, followed by an uncharacterized region, prior to the C-terminal tandem array of 11 fingers (Figure 1B). We generated two constructs, residues 1–105 containing the first

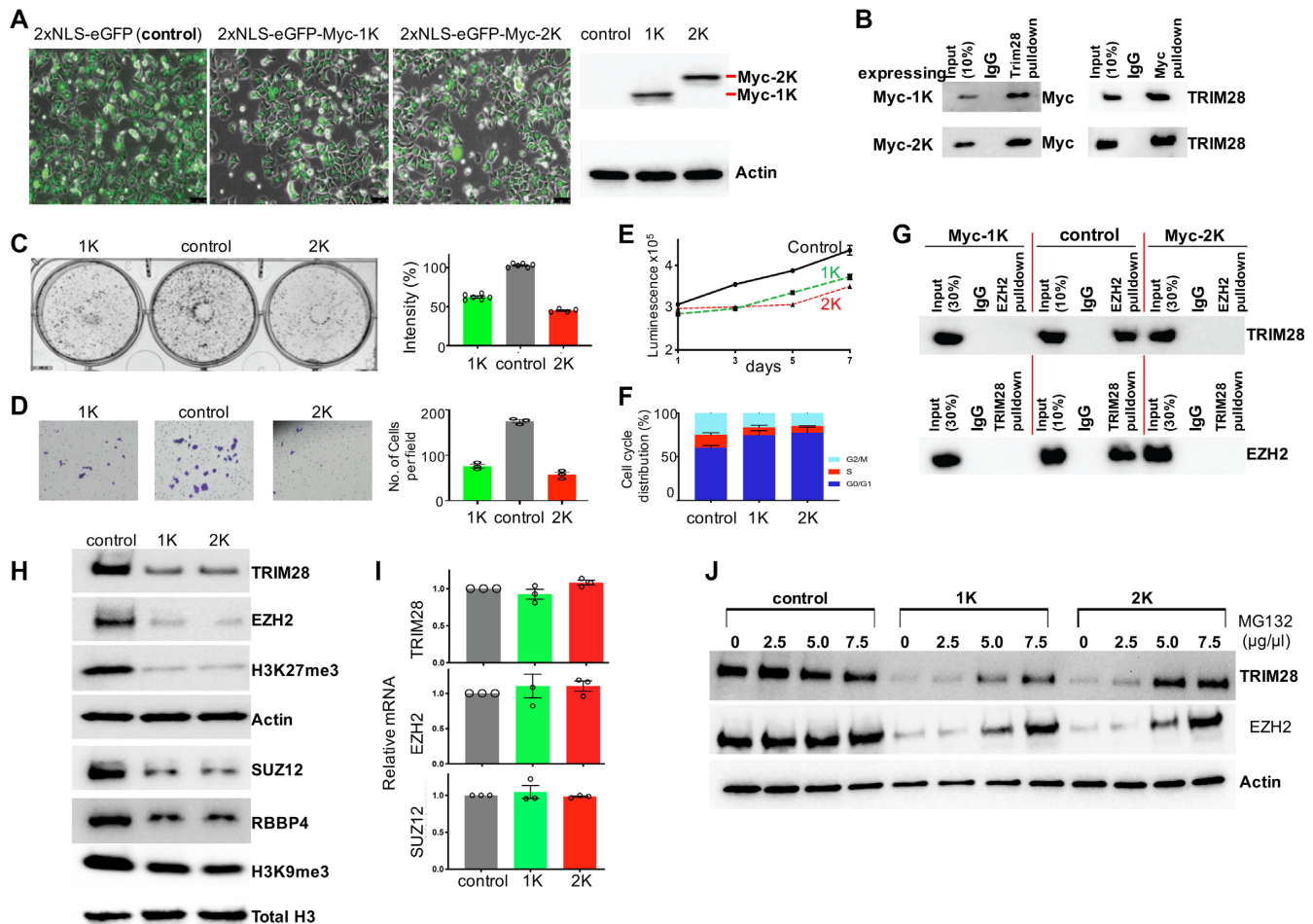


Figure 2. KRAB domain disrupts TRIM28–EZH2 interactions. (A) Expression of 1K and 2K assessed in the construct of 2xNLS-eGFP-Myc by GFP expression and western blot against Myc in MCF7 cells. (B) TRIM28 and Myc-1K or Myc-2K were subjected to immunoprecipitations and immunoblotting with TRIM28 and Myc antibodies. The inhibitory growth effect of 1K and 2K shown by (C) colony formation assay, (D) Transwell migration assay, (E) cell viability assay and (F) cell cycle analysis. (G) Endogenous EZH2 and TRIM28 were immunoprecipitated in cells expressing Myc-1K or Myc-2K and subjected to immunoblotting with TRIM28 and EZH2 antibodies. (H) Western blot showing the endogenous levels of TRIM28, EZH2, H3K27me3, SUZ12 and RBBP4. (I) Relative gene expressions of TRIM28, EZH2 and SUZ12 in MCF7 cells with Myc-1K or Myc-2K expression were analyzed by qRT-PCR and normalized relative to IP08. (J) MCF7 cells were treated with MG132 with indicated concentrations for 24 h and subjected to immunoblot. Data represent mean \pm SEM of three independent determinations ($N = 3$) and blots are representative of one experiment.

KRAB domain (termed 1K) and residues 1–360 of the entire N-terminal fragment containing both KRAB domains (termed 2K). Recombinant proteins of KRAB-containing fragments (either 1K or 2K) and TRIM28 (full-length or N-terminal RBCC domain) co-expressed in *E. coli* form stable complexes (Supplementary Figure S1A and B). We used three biophysical methods to measure the absolute mass of the complex of RBCC:1K. First, the samples were subjected to size-exclusion chromatography coupled with synchrotron multi-angle light scattering (46), which gave the absolute mass of 154 kDa (Figure 1C and Supplementary Figure S1C and D). The same fractions eluted from the size-exclusion chromatography were simultaneously examined by synchrotron small-angle X-ray scattering (SAXS) (47), which gave the molecular weight of 157 kDa and the maximum dimension of the complex to be ~ 234 Å long (Figure 1C and D, and Supplementary Figure S1E–I). The elongated overall shape of the SAXS model agrees with X-ray crystal structures of TRIM28 RBCC fragment (19,20)

(Figure 1D). We assume the additional unaccounted density near the center of the SAXS envelope might be where the KRAB domain bound (Figure 1D). Finally, sedimentation velocity analytical ultracentrifugation studies revealed the existence of two populations, one at 159 kDa (in agreement with the two scattering methods) and the second at 312 kDa (nearly double the size of the first population) (Figure 1C and E). The ratio between the two populations did vary among preparations.

Our observed molecular mass at ~ 160 kDa agrees well with the original observation that TRIM28 RBCC forms trimers and binds the KRAB domain with a stoichiometry of 3:1 (11,48) or 3:2 (Figure 1C). Only when we mutated a surface residue of the B1 box (Figure 1D), arginine 184 to aspartate (R184D), the dominant population at mass of 97.5 kDa matches well with a stoichiometry of 2:1 (Figure 1C and F). It is still debatable in the literature whether TRIM28 (full length or RBCC) forms high-order oligomers (14,19,20,49), which might depend on the protein concen-

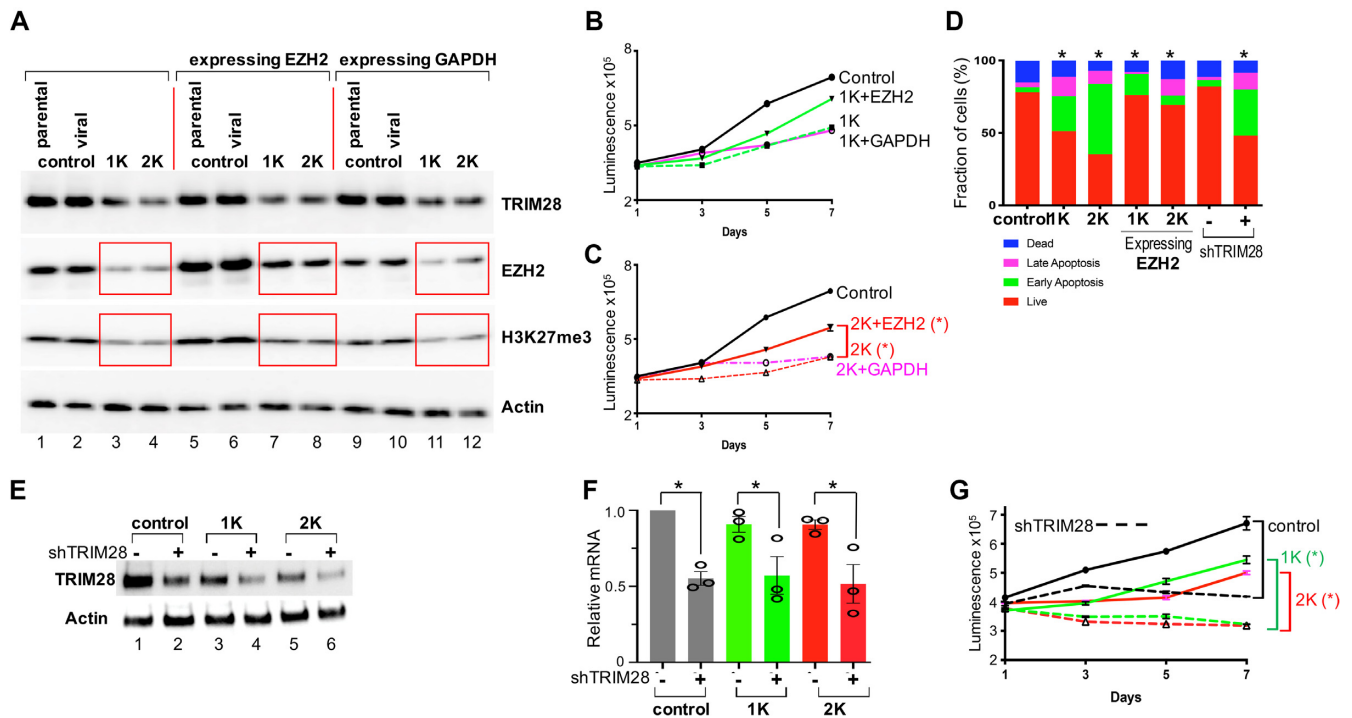


Figure 3. EZH2 overexpression partially rescues growth defect. (A) Western blot confirms increased level of EZH2, H3K27me3 with no change in TRIM28 and actin was used as a control. (B, C) Partial rescue of cell growth as shown by cell viability assay over a period of 7 days. (D) Apoptosis assay. Percentage of apoptosis for the indicated cell lines. (E) Western blot showing the endogenous levels of TRIM28, confirming knockdown by shTRIM28 and actin was used as a loading control. (F) Relative gene expressions of TRIM28 in the presence or absence of shTRIM28 knockdown were analyzed by qRT-PCR and normalized relative to IPO8. (G) The inhibitory growth effect of knockdown TRIM28 shown by cell viability assay. Data represent mean \pm SEM of three independent determinations ($N = 3$) and an asterisk indicates $P < 0.05$ compared to the control.

tration range tested under varied laboratory conditions (see the ‘Discussion’ section in the Supplementary Data). In addition, introducing the chato mutation (50,51) in the context of ZFP568 1K and 2K fragments significantly reduced interactions with Trim28 in the pull-down assay (Supplementary Figure S2).

Expression of KRAB domain in MCF7 interrupts TRIM28–EZH2 interactions and slows cell growth

We next developed MCF7 cell lines that stably express 1K or 2K as eGFP–Myc fusion constructs and confirmed overexpression by eGFP fluorescence and Myc detection (Figure 2A). Co-immunoprecipitation (co-IP) of endogenous TRIM28 with KRAB fusion proteins confirmed the interaction of TRIM28 with KRAB-containing fragments 1K and 2K (Figure 2B). MCF7 cells with stably expressed 1K or 2K protein grew significantly slower than control cells (Figure 2C) with decreased cell migration (Figure 2D). The 2K expression had a stronger inhibitory effect assessed by colony formation assay (Figure 2C) and cell proliferation assay (Figure 2E) over a period of 7 days. The cells showed a growth arrest at G0/G1 analyzed by cell cycle (Figure 2F). We note that some proteins that could contribute to these phenotypic changes, such as cyclin D1 and BCL2, were downregulated with an increased BAX/BCL2 ratio [a marker for apoptosis (52,53)], as revealed by both RNA-seq and reverse-phase protein lysate microarray (RPPA) assay (54) (Supplementary Figure S3F).

It was previously reported that in MCF7 cells, TRIM28 interacts with EZH2 (33), a member of the polycomb repressor 2 (PRC2) complex (Figure 2G, control lanes). As we hypothesized, the interaction between TRIM28 and EZH2 is totally disrupted in MCF7 lines stably expressing KRAB domains (Figure 2G, lanes with Myc-1K or Myc-2K). Unexpectedly, we found that endogenous protein levels of EZH2 and TRIM28 are drastically reduced (Figure 2H), a finding confirmed by RPPA analysis (TRIM28 in Supplementary Figure S3F). Consistent with the loss of EZH2, the sole histone methyltransferase that catalyzes the trimethylation of histone H3 lysine 27 (H3K27me3) (55), total histone H3K27me3 levels and other components of PRC2 complex (SUZ12 and RBBP4) were also reduced (Figure 2H). We note that H3K9me3 level is also reduced to some extent (Figure 2H), probably via the TRIM28-associated histone methyltransferase SETDB1.

In contrast, the mRNA levels of TRIM28, EZH2 and SUZ12 remained unaltered in KRAB-expressing cells, compared to control cells (Figure 2I), suggesting the reduction in protein levels of PRC2 components was not at the transcriptional level. Next, we treated the cells with proteasome inhibitor (MG132) for 24 h and assessed protein levels of TRIM28 and EZH2 in cells expressing KRAB domains (Figure 2J). Whereas TRIM28 and EZH2 protein levels in control cells changed little with MG132 treatment, both 1K- and 2K-expressing cells exhibited significantly increased levels of TRIM28 and EZH2 in a concentration-dependent manner, suggesting that the two proteins were

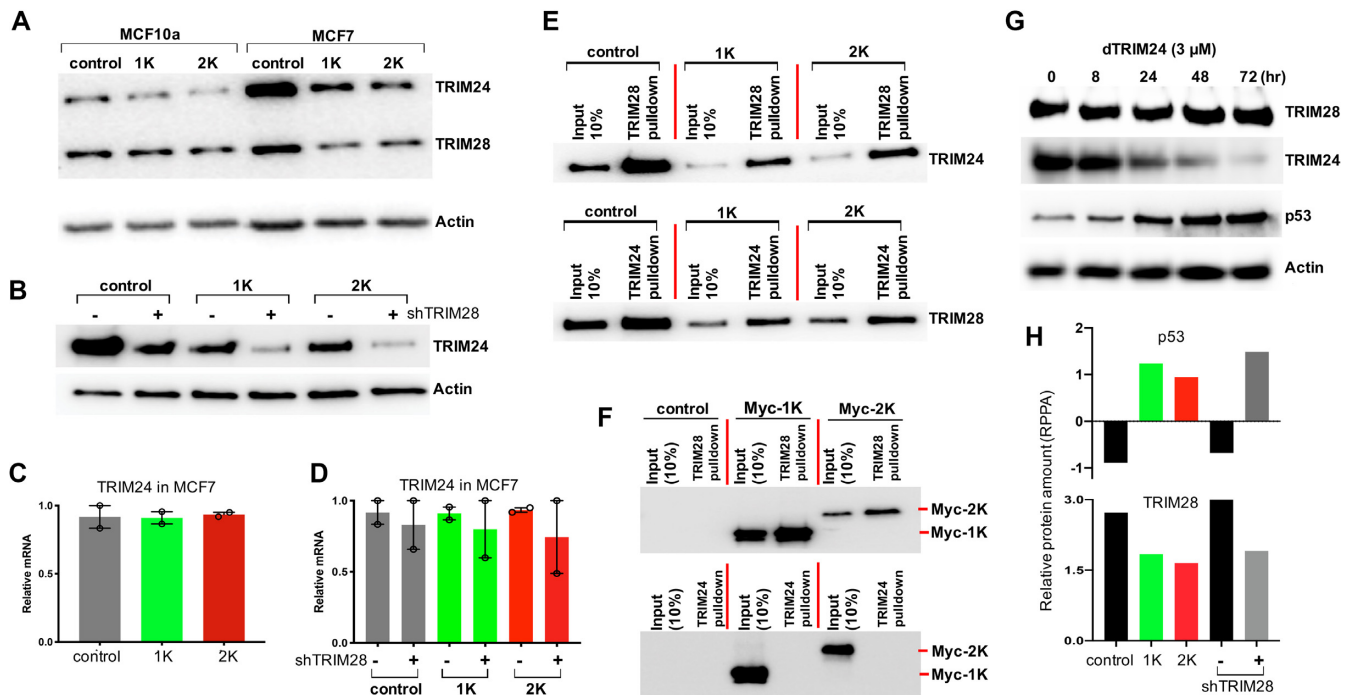


Figure 4. KRAB domain interacts with TRIM28 but not TRIM24. (A) Endogenous levels of TRIM24 and TRIM28 shown by immunoblot. (B) Western blot shows endogenous levels of TRIM24 in shTRIM28 cells. (C, D) Relative mRNA expression of TRIM24 normalized against IPO8 by qRT-PCR in the absence and presence of shTRIM28. (E) Endogenous TRIM24 and TRIM28 were immunoprecipitated in cells expressing Myc-1K or Myc-2K. (F) TRIM28, but not TRIM24, interacts with KRAB. (G) TRIM24 degrader (dTRIM24) decreased TRIM24 and increased p53 protein level but not TRIM28. (H) Increased p53 protein level in RPPA analysis.

degraded by MG132-sensitive proteasome machinery in KRAB-expressing cells.

Expressing EZH2 in KRAB-expressing cells partially restores growth rate

To test whether the reduced level of EZH2 is responsible for growth repression by KRAB domain expressing cells, we overexpressed EZH2 in these cells with GAPDH as a negative control. Western blot analyses showed that overexpressing EZH2 in 1K or 2K cells (lanes 7 and 8 in Figure 3A) restored the level of EZH2 to that of parental MCF7 cells (lane 1), while the level of H3K27me3 was only partially restored and TRIM28 remained largely unchanged (Figure 3A). As a result, the rate of proliferation (Figure 3B and C) and the fraction of live cells (Figure 3D) were partially restored to parental cell levels.

Due to the unexpected reduction of TRIM28 protein level in KRAB-expressing cells, we set out to compare the effect of KRAB expression with that of a TRIM28 knockdown (shRNA) MCF7 cell line. The reduction of TRIM28 in shTRIM28 line was confirmed by western blot and relative mRNA levels (Figure 3E and F). We noted that the TRIM28 level in shTRIM28 line is comparable to the 2K-expressing line (Figure 3E, compare lanes 2 and 5), and that the shTRIM28 line has similarly reduced growth rate to that of the 2K-expressing cell line (Figure 3G). Interestingly, further reduction of TRIM28 level in 1K- and 2K-expressing cells by shTRIM28 (Figure 3E) caused complete inhibition

of growth (Figure 3G), such that the cell lines could not be established beyond two passages.

KRAB interacts with TRIM28, but not TRIM24

TRIM24, a related member of TRIM family, is an oncogene when aberrantly overexpressed (56). In prostate cancer, TRIM28 interacts with TRIM24 to prevent its degradation (24). We asked whether TRIM24 levels could also be affected in MCF7 cells expressing KRAB domains, as a result of degradation of TRIM28 proteins. Indeed, TRIM24 protein levels are significantly reduced in cells expressing KRAB (Figure 4A) or knockdown of TRIM28 (shTRIM28) (Figure 4B), whereas there is little change at the transcriptional level of TRIM24 (Figure 4C and D).

We confirmed that TRIM24 and TRIM28 interact with each other by co-IP (Figure 4E, control lanes). Unlike TRIM28–EZH2 interaction, TRIM28–TRIM24 interaction is not affected by the presence of KRAB domain expression (Figure 4E). Although TRIM24 and TRIM28 are closely related family members (57), TRIM24 does not interact with KRAB domains, unlike TRIM28 (Figure 4F), suggesting that the TRIM28 uses two distinct interfaces for KRAB and TRIM24 interactions and forms two distinct non-overlapping complexes (TRIM28–TRIM24 and TRIM28–KRAB).

A small-molecule TRIM24 degrader (dTRIM24) that conjugates TRIM24 bromodomain to an E3 ubiquitin ligase is available to target TRIM24 to degradation (58). Treat-

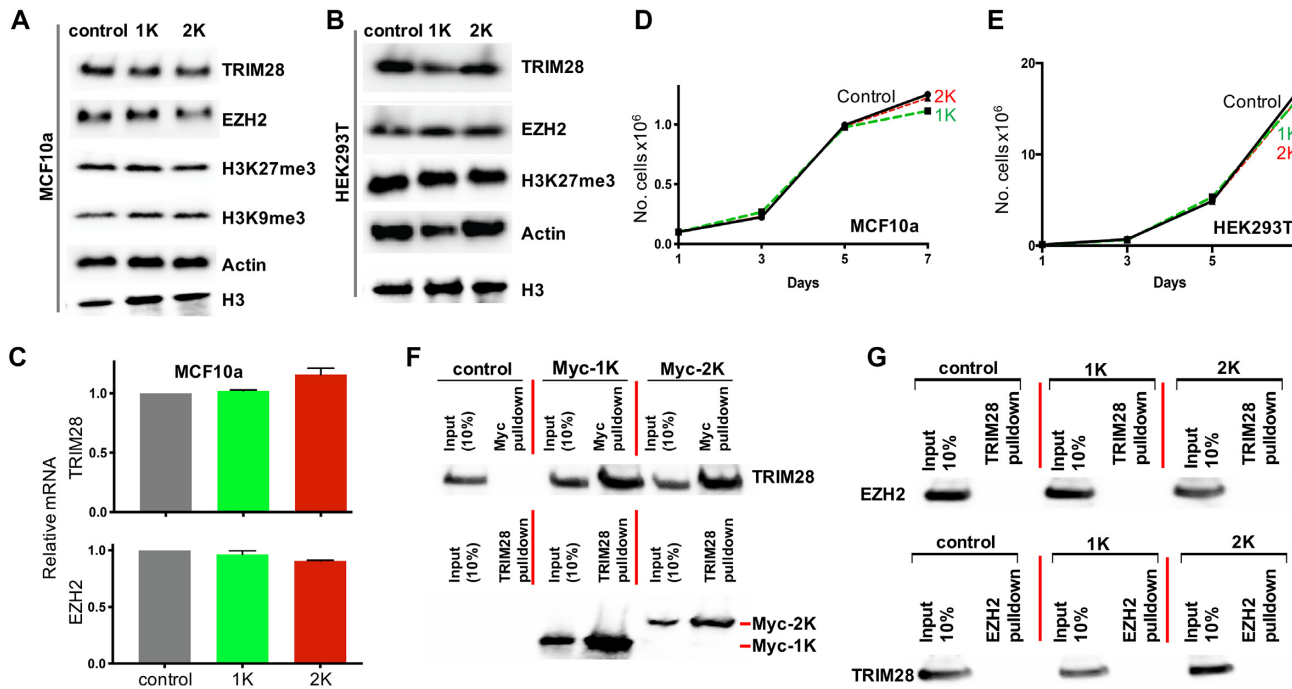


Figure 5. Expression of KRAB domain has minimal effect in MCF10a and HEK293T cells. Endogenous protein levels of TRIM28, EZH2, H3K27me3 and H3K9me3 with Actin and total H3 as a loading control by immunoblotting in MCF10a (A) and HEK293T cells (B). (C) Cells that express Myc-1K or Myc-2K in MCF10a cells showed no change in relative mRNA levels of TRIM28 and EZH2 in MCF10a cells. (D, E) No change in cell growth. (F) Endogenous TRIM28 interacts with Myc-1K or Myc-2K in MCF10a cells. (G) No interaction between EZH2 and TRIM28 in MCF10a cells.

ment of MCF7 cells with dTRIM24 at 3 μ M resulted in decreased TRIM24 protein with no change in TRIM28 (Figure 4G), confirming TRIM28 is upstream of TRIM24 (24). Consistent with TRIM24 directly ubiquitylating p53 for degradation (36,37), we observed that the levels of p53 increased along with decreased TRIM24 protein levels (Figure 4G). Similarly, we also observed an increase in p53 protein level in an RPPA assay of cells expressing KRAB domain (Figure 4H).

KRAB domain expression has minimal effect on non-cancerous cells

We also expressed KRAB domains in non-tumor-derived cells, including MCF10a immortalized, non-transformed human mammary epithelial cells and human embryonic kidney HEK293T cells, to assess whether the effect of KRAB expression is specific to tumor-derived cells. We first noticed that the protein levels of TRIM28 and TRIM24 were not affected in MCF10a (Figure 4A) or HEK293T cells with the expression of KRAB domains. Similarly, there is no significant change at the protein (Figure 5A and B) or transcriptional level (Figure 5C) for TRIM28, EZH2 and associated histone modification H3K27me3. More importantly, the MCF10a and HEK293T cells expressing KRAB domain exhibit no growth defects (Figure 5D and E). Co-IP showed that the expressed KRAB domains do interact with TRIM28 in MCF10a cells (Figure 5F), as in the case of MCF7, but there is no interaction between TRIM28 and EZH2 (Figure 5G).

Genome-wide gene expression changes of KRAB zinc finger proteins induced by 2K expression

To obtain a genome-wide view of the gene expression changes induced by KRAB domain expression, we performed RNA sequencing on MCF7 cells expressing KRAB domains and vector control cells, as well as shTRIM28 cells with shControl. Principal component analysis indicated that the two biological replicates of each sample clustered together by groups (control, 1K, 2K, shControl, shTRIM28) (Supplementary Figure S3A). Overall, there were 6333 genes differentially expressed in 2K-expressing cells, 282 in 1K-expressing cells relative to control and 4191 genes in shTRIM28 cells relative to the shControl (by false discovery rate ≤ 0.05). Similar to colony formation and cell proliferation assays (Figure 2), the 2K expression affected a larger number of genes. The majority of genes changed in the 1K dataset (201/282) overlapped with those of the 2K, including 127 upregulated (51 of them are KRAB-ZF genes) and 74 downregulated. We thus focus on comparison of the 2K datasets with that of shTRIM28.

Using cutoffs of false discovery rate ≤ 0.05 and fold change ≥ 2 , the 2K-expressing cells had 1197 genes significantly altered, of which 801 genes were downregulated and 396 genes were upregulated (Supplementary Figure S3B). For comparison, 612 genes were significantly altered in shTRIM28, with 425 upregulated and 187 downregulated (Supplementary Figure S3C). QIAGEN's Ingenuity Pathway Analysis showed the top altered gene ontologies enriched in control versus 2K and ShControl versus ShTRIM28 are important for cell death and survival, cellu-

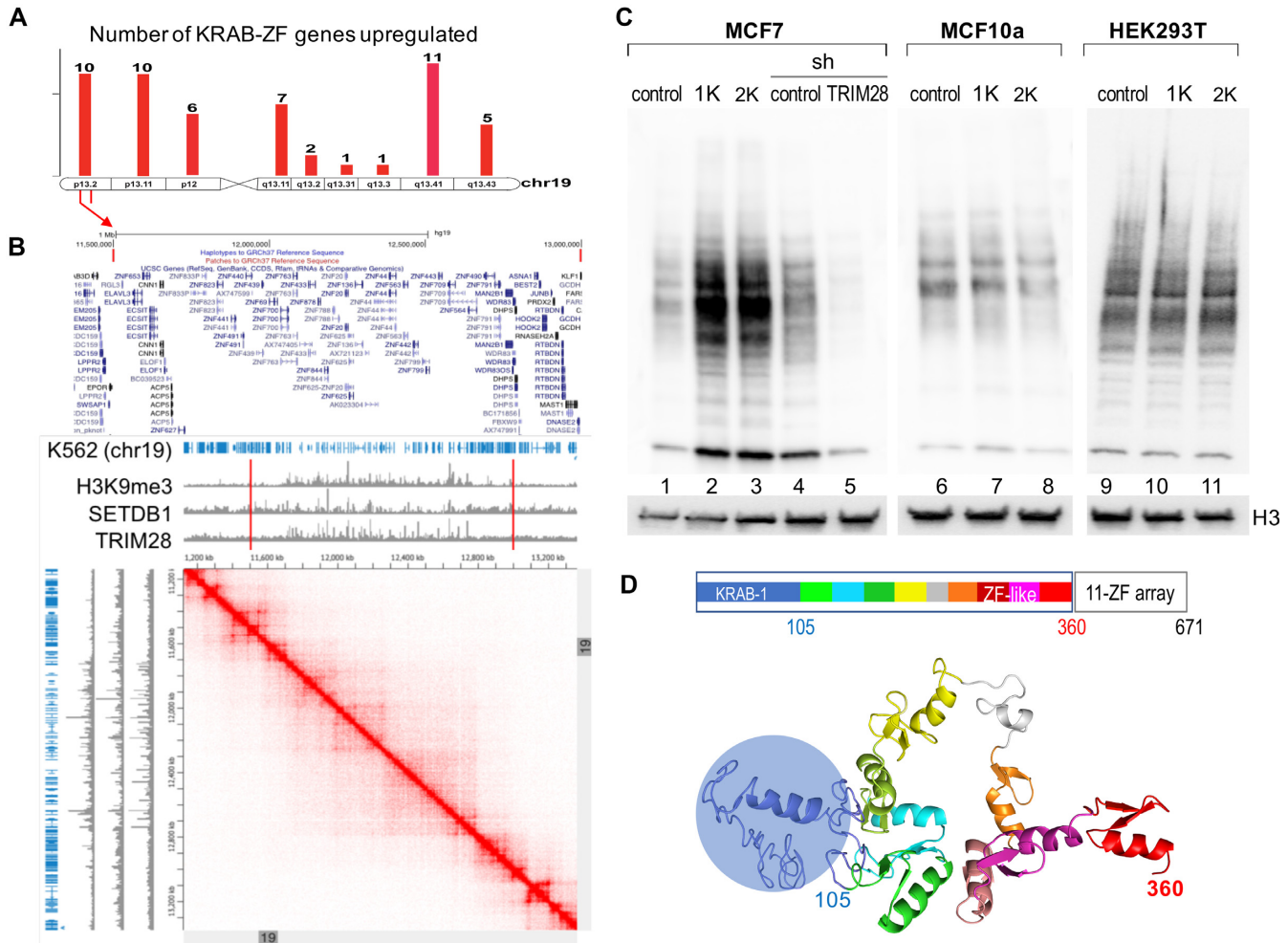


Figure 6. Upregulation of KRAB-ZF genes in chromosome 19. (A) Upregulation of 53 KRAB-ZF genes in chromosome 19 (see Supplementary Table S2). (B) Genome browser views of HiC (GSE63525), H3K9me3 (ENCODE: ENCSR000APE), SETDB1 (ENCODE: ENCSR000EWI) and TRIM28 (ENCODE: ENCSR474CVP) ChIP-seq signals from human K562 cells within the KRAB-ZF cluster (chromosome 19: 11 055 001–13 295 000) indicated by two vertical red lines. The heat map was generated using Juicebox. (C) Western blot showing the endogenous levels of ZF proteins. (D) A predicted model of the 2K fragment (residues 1–360) of mouse ZFP568.

lar growth and proliferation, cellular development and cell movement (Supplementary Figure S3D and E), although with different numbers of genes in each category. Examples of alteration in gene expression are consistent with the protein levels of the same genes analyzed by RPPA (Supplementary Figure S3F).

Unexpectedly, of the 400 genes that were upregulated with fold change ≥ 2 in the 2K-expressing cells, the greatest number of them were 63 KRAB-ZF genes, 53 of which are on chromosome 19 (Figure 6A and B, and Supplementary Table S2). The increased expression of ZF proteins was confirmed by western blot using an antibody generated against the ZF linker region (27) (Figure 6C). However, the changes in KRAB-ZF gene expression were not seen with knock-down shTRIM28 line, despite that the remaining protein levels of TRIM28 were similar in the shTRIM28 cells and the 1K- or 2K-expressing cells ($\sim 60\%$ of control; comparing lanes 2, 3 and 5 in Figure 3E). In fact, the overall KRAB-ZF protein level in shTRIM28 MCF7 cells was significantly reduced, perhaps due to increased degradation as a result

of reduced TRIM28 level, as was observed in other breast cancer cells (27). Homology modeling of the 2K fragment of mouse ZFP568 suggested the existence of at least eight ZF-like units, each comprising two β -strands and a helix, after the first KRAB domain (Figure 6D). We speculate that the presence of KRAB domain prevents the remaining TRIM28 from repressing the expression of many KRAB-ZF genes (see the ‘Discussion’ section in the Supplementary Data).

DISCUSSION

Across primary human breast cancers in the Cancer Genome Atlas (TCGA) (59), TRIM28 is highly expressed whereas ZFP568 is consistently low expressed (Supplementary Figure S4). Here, we showed that introducing a peptide fragment containing the KRAB domain of ZFP568 into MCF7 cells led to changes in protein levels of TRIM28, TRIM24, EZH2 (and other PRC2 complex components), p53 and KRAB-ZF proteins (Figure 7). We find that the

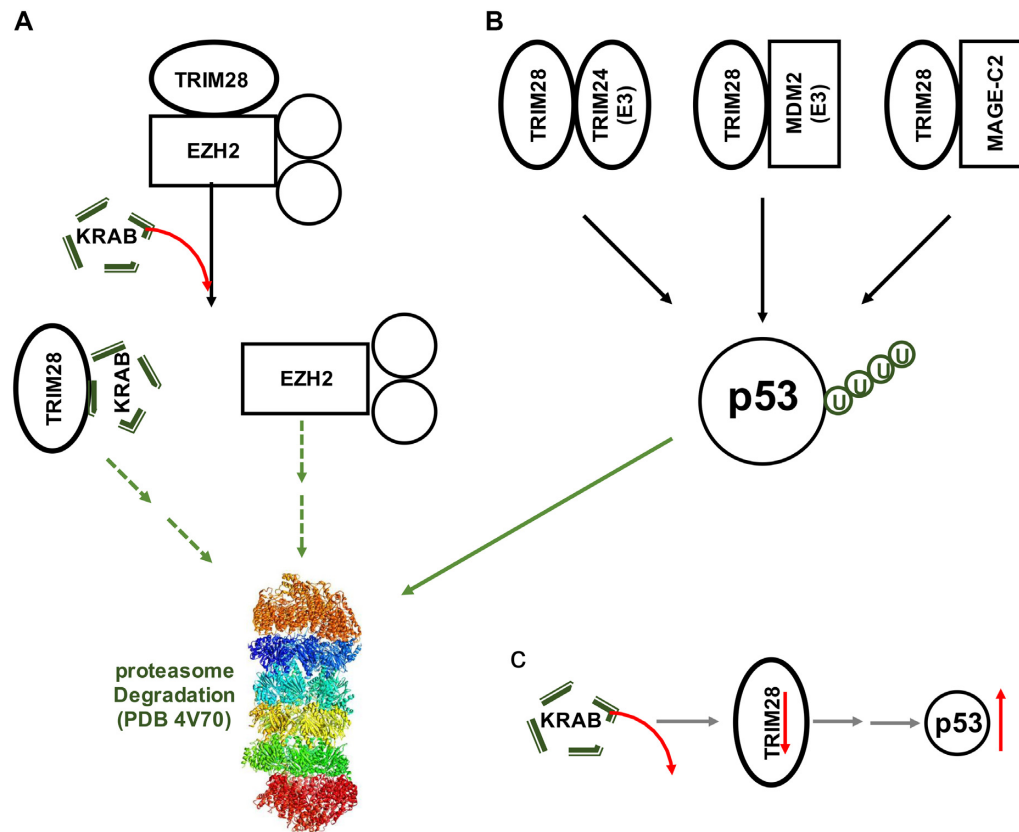


Figure 7. Potential models of introducing a KRAB domain in MCF7 cells. (A) Disruption of TRIM28–EZH2 interaction leads to degradation of both proteins. (B, C) Reduced TRIM28 protein level leads to reduced E3 ligases (TRIM24 and MDM2), decreased p53 ubiquitination and increased p53 protein level.

KRAB domain competes with and disrupts TRIM28–EZH2 interactions and significantly reduced the protein levels of TRIM28 and EZH2 through proteasome-mediated degradation. The reason for TRIM28 protein degradation is not clear. One speculation is that the overexpressed KRAB domain binds to TRIM28, but the complex is unable to bind DNA, therefore not incorporated into the heterochromatin complex that TRIM28 normally belongs. The non-chromatin-associated TRIM28–KRAB complex is perhaps more susceptible to proteasome degradation (Figure 7A). The same could be said for the TRIM28-bound EZH2 that is displaced by KRAB domain from chromatin. MCF7 cells stably expressing KRAB domain showed decreased proliferation and migration, increased apoptosis and cell cycle arrest at G0/G1, all of which can be partially rescued by overexpressing EZH2. We note that a number of EZH2 small-molecule inhibitors have been developed targeting its enzymatic activity (60). Disrupting TRIM28–EZH2 interaction might provide a novel mechanism to suppress EZH2 function in cancer cells by degrading EZH2 protein and thus ultimately diminishing its enzyme activity—which could potentially expand the therapeutic niche of drug combinations, overcoming resistance that may develop toward existing EZH2 inhibitors.

We note that existing EZH2 inhibitors that do not affect EZH2 protein levels in cells are ineffective at blocking proliferation of triple negative (for ER, PR and HER2)

breast cancer cells even though they effectively reduce the H3K27me3 mark (61,62). However, knockdown of EZH2 via RNA interference is sufficient to block tumor growth (63). Interestingly, we observed more severe inhibitory effect by KRAB expression on cell growth of triple negative MDA-MB231 cells, where stable lines could not be established beyond the first passage upon introducing the KRAB domain containing 1K or 2K fragment (Supplementary Figure S5A). We did observe decreased EZH2 protein level as well as H3K27me2 mark in the first passage cells (Supplementary Figure S5B–E). A recent report of an EZH2-selective degrader (64) showed a cytotoxic effect in multiple triple negative breast cancer cells, while sparing normal cells, and is efficacious *in vivo*. This observation and our study suggest that pharmacological degradation of EZH2 protein can be advantageous for treating the cancers that are dependent on non-catalytical functions of EZH2. We also note that catalytically activating mutations in EZH2 (65) are significantly enriched in germinal center B-cell-like lymphoma, where EZH2 inhibitors have been shown to be clinically effective (66). Strategies to reduce EZH2 protein level could potentially be synergistic or additive to EZH2 inhibitor therapy.

There are at least three TRIM28-associated protein complexes identified that target p53 for ubiquitination and degradation: TRIM24 (24,36,37), MDM2 (34) and MAGE-C2 (38) (Figure 7B). MDM2, TRIM24 or TRIM28 each

contains a RING domain that could act as ubiquitin or SUMO E3 ligases. Indeed, MDM2 and TRIM24 have been shown to ubiquitylate p53 directly (34,36,37), whereas the isolated RING domain of TRIM28 lacks activity (67) but MAGE-TRIM28 interactions reportedly form an active ubiquitin ligase (31,68,69). Meanwhile, TRIM28 undergoes auto-SUMOylation, which promotes its protein-protein interactions (70,71). As a scaffolding protein that forms dimer or trimer or even higher order oligomers, TRIM28-mediated interaction with TRIM24, MDM2 and MAGE-C2 could co-exist in a large complex. As shown, introducing ectopic KRAB domains decreased TRIM28 level, which also brings down the levels of TRIM24 and, potentially, MDM2 (Supplementary Figure S3F) or MAGE-C2 (40). The net result is decreased ubiquitination of p53, and thus increased level of p53 protein (Figure 7C). Regulation of tumor suppressor p53 is essential for maintenance of genome integrity (72,73), innate immune response (74), stem cells and development (75). Interestingly, as a feedback regulation, MDM2 and members of TRIM family are high-confidence p53 target genes (76). We suggest that targeting TRIM28, and associated E3 ligases, could be developed into next-generation modulators as p53 therapeutics. A potent small-molecule inhibitor, idasanutlin (RG7388), that disrupts MDM2-p53 interaction is being clinically investigated for many cancers, including relapse/refractory acute myeloid leukemia patients (77-79).

Based on our data and prior observations in the literature, we suggest that in cancer cells where significant upregulation of TRIM28 occurs, introducing peptides containing KRAB domain (or a small-molecule interrupter) into the cell might prevent TRIM28 from abnormal interactions with other transcription regulators, and possibly counter the pro-tumorigenic effect of TRIM28. Mechanistically, we showed that TRIM28 depletion results in proteasome-dependent degradation of EZH2, increased protein stability of tumor suppressor p53 and increased expression of multiple KRAB-ZF proteins. These findings demonstrate that TRIM28 and KRAB-ZF proteins may play an important role in breast cancer and could be explored as targets for therapeutic intervention.

DATA AVAILABILITY

The RNA-seq data have been deposited in the GEO database (accession number: GSE146769).

SUPPLEMENTARY DATA

Supplementary Data are available at NAR CANCER Online.

ACKNOWLEDGEMENTS

We thank Yiwei Liu, Yusef Olatunde Olanrewaju, Suparna Bhattacharya and Zhongwu Zhou for their participation in initial work of preparing expression constructs and protein purifications. We thank Dr B.V. Venkatar Prasad and Dr Soni Kaundal of Baylor College of Medicine for helping in sedimentation velocity analytical ultracentrifugation experiments and Dr Paul A. Wade of National Institute

of Environment Health Sciences for discussion. We thank Dr Mien-Chie Hung of MD Anderson Cancer Center for MCF7, MCF10a and HEK293T cells.

Author contributions: X.Z. conceived the initial concept; J.K. performed all cell-based experiments; G.K. performed biophysical experiments and homology modeling; G.K. and R.R. purified recombinant proteins used in the biophysical experiments; Y.L. and K.L. performed bioinformatics analysis of RNA-seq data; J.L. and Y.H. analyzed ENCODE data on K562 cells; A.P. performed *in vitro* pull-down assay; M.C.B. participated in discussion throughout; T.M. provided initial ZFP568 constructs and participated in discussion; X.Z. and X.C. organized and designed the scope of the study. All were involved in preparing the manuscript.

FUNDING

Cancer Prevention Research Institute of Texas [RR160029 to X.C., who is a CPRIT Scholar in Cancer Research. RP170002 supports the NGS sequencing core]; National Institutes of Health [R35GM134744 to X.C., R01HL134780 and R01HL146852 to J.L. and Y.H., 1R01CA214871 to M.C.B., 1ZIAHD008933 to T.M., P30CA016672-40 supports the Functional Proteomics RPPA core facility at the MD Anderson Cancer Center, P30GM124169-01 supports SAXS data collection at SIBYLS]; American Cancer Society [RSG-18-043-01-LIB to J.L. and Y.H.]; Department of Energy's Office of Biological and Environmental Research, Integrated Diffraction Analysis Technology Program.

Conflict of Interest statement. None declared.

REFERENCES

- Vinogradov, A.E. (2012) Human more complex than mouse at cellular level. *PLoS One*, **7**, e41753.
- Imbeault, M., Helleboid, P.Y. and Trono, D. (2017) KRAB zinc-finger proteins contribute to the evolution of gene regulatory networks. *Nature*, **543**, 550-554.
- Helleboid, P.Y., Heusel, M., Duc, J., Piot, C., Thorball, C.W., Coluccio, A., Pontis, J., Imbeault, M., Turelli, P., Aebbersold, R. *et al.* (2019) The interactome of KRAB zinc finger proteins reveals the evolutionary history of their functional diversification. *EMBO J.*, **38**, e101220.
- Seah, M.K.Y., Wang, Y., Goy, P.A., Loh, H.M., Peh, W.J., Low, D.H.P., Han, B.Y., Wong, E., Leong, E.L., Wolf, G. *et al.* (2019) The KRAB-zinc-finger protein ZFP708 mediates epigenetic repression at RMR19B retrotransposons. *Development*, **146**, dev170266.
- Wolf, G., de Laco, A., Sun, M.-A., Bruno, M., Tinkham, M., Hoang, D., Mitra, A., Ralls, S., Trono, D. and Macfarlan, T. (2020) Non-essential function of KRAB zinc finger gene clusters in retrotransposon suppression. bioRxiv doi: <https://doi.org/10.1101/2020.01.17.910679>, 17 January 2020, preprint: not peer reviewed.
- Baudat, F., Buard, J., Grey, C., Fledel-Alon, A., Ober, C., Przeworski, M., Coop, G. and de Massy, B. (2010) PRDM9 is a major determinant of meiotic recombination hotspots in humans and mice. *Science*, **327**, 836-840.
- Quenneville, S., Verde, G., Corsinotti, A., Kapopoulou, A., Jakobsson, J., Offner, S., Baglivo, I., Pedone, P.V., Grimaldi, G., Riccio, A. *et al.* (2011) In embryonic stem cells, ZFP57/KAP1 recognize a methylated hexanucleotide to affect chromatin and DNA methylation of imprinting control regions. *Mol. Cell*, **44**, 361-372.
- Yang, P., Wang, Y., Hoang, D., Tinkham, M., Patel, A., Sun, M.A., Wolf, G., Baker, M., Chien, H.C., Lai, K.N. *et al.* (2017) A placental growth factor is silenced in mouse embryos by the zinc finger protein ZFP568. *Science*, **356**, 757-759.
- Urrutia, R. (2003) KRAB-containing zinc-finger repressor proteins. *Genome Biol.*, **4**, 231.

10. Liu, Y., Zhang, X., Blumenthal, R.M. and Cheng, X. (2013) A common mode of recognition for methylated CpG. *Trends Biochem. Sci.*, **38**, 177–183.
11. Peng, H., Begg, G.E., Schultz, D.C., Friedman, J.R., Jensen, D.E., Speicher, D.W. and Rauscher, F.J. 3rd (2000) Reconstitution of the KRAB-KAP-1 repressor complex: a model system for defining the molecular anatomy of RING-B box-coiled-coil domain-mediated protein-protein interactions. *J. Mol. Biol.*, **295**, 1139–1162.
12. Friedman, J.R., Fredericks, W.J., Jensen, D.E., Speicher, D.W., Huang, X.P., Neilson, E.G. and Rauscher, F.J. 3rd (1996) KAP-1, a novel corepressor for the highly conserved KRAB repression domain. *Genes Dev.*, **10**, 2067–2078.
13. Ozato, K., Shin, D.M., Chang, T.H. and Morse, H.C. 3rd (2008) TRIM family proteins and their emerging roles in innate immunity. *Nat. Rev. Immunol.*, **8**, 849–860.
14. Sun, Y., Keown, J.R., Black, M.M., Raclot, C., Demarais, N., Trono, D., Turelli, P. and Goldstone, D.C. (2019) A dissection of oligomerization by the TRIM28 tripartite motif and the interaction with members of the Krab-ZFP family. *J. Mol. Biol.*, **431**, 2511–2527.
15. Schultz, D.C., Ayyanathan, K., Negorev, D., Maul, G.G. and Rauscher, F.J. 3rd (2002) SETDB1: a novel KAP-1-associated histone H3, lysine 9-specific methyltransferase that contributes to HP1-mediated silencing of euchromatic genes by KRAB zinc-finger proteins. *Genes Dev.*, **16**, 919–932.
16. Ryan, R.F., Schultz, D.C., Ayyanathan, K., Singh, P.B., Friedman, J.R., Fredericks, W.J. and Rauscher, F.J. 3rd (1999) KAP-1 corepressor protein interacts and colocalizes with heterochromatic and euchromatic HP1 proteins: a potential role for Kruppel-associated box-zinc finger proteins in heterochromatin-mediated gene silencing. *Mol. Cell. Biol.*, **19**, 4366–4378.
17. Schultz, D.C., Friedman, J.R. and Rauscher, F.J. 3rd (2001) Targeting histone deacetylase complexes via KRAB-zinc finger proteins: the PHD and bromodomains of KAP-1 form a cooperative unit that recruits a novel isoform of the Mi-2alpha subunit of NuRD. *Genes Dev.*, **15**, 428–443.
18. Quenneville, S., Turelli, P., Bojkowska, K., Raclot, C., Offner, S., Kapopoulou, A. and Trono, D. (2012) The KRAB-ZFP/KAP1 system contributes to the early embryonic establishment of site-specific DNA methylation patterns maintained during development. *Cell Rep.*, **2**, 766–773.
19. Stoll, G.A., Oda, S.I., Chong, Z.S., Yu, M., McLaughlin, S.H. and Modis, Y. (2019) Structure of KAP1 tripartite motif identifies molecular interfaces required for retroelement silencing. *Proc. Natl Acad. Sci. U.S.A.*, **116**, 15042–15051.
20. Lim, M., Newman, J.A., Williams, H.L., Masino, L., Aitkenhead, H., Gravard, A.E., Gileadi, O. and Svejstrup, J.Q. (2019) A ubiquitin-binding domain that binds a structural fold distinct from that of ubiquitin. *Structure*, **27**, 1316–1325.
21. Zeng, L., Yap, K.L., Ivanov, A.V., Wang, X., Mujtaba, S., Plotnikova, O., Rauscher, F.J. 3rd and Zhou, M.M. (2008) Structural insights into human KAP1 PHD finger-bromodomain and its role in gene silencing. *Nat. Struct. Mol. Biol.*, **15**, 626–633.
22. Cammas, F., Mark, M., Dolle, P., Dierich, A., Chambon, P. and Losson, R. (2000) Mice lacking the transcriptional corepressor TIF1beta are defective in early postimplantation development. *Development*, **127**, 2955–2963.
23. Rousseaux, M.W., Revelli, J.P., Vazquez-Velez, G.E., Kim, J.Y., Craigen, E., Gonzales, K., Beckinghausen, J. and Zoghbi, H.Y. (2018) Depleting Trim28 in adult mice is well tolerated and reduces levels of alpha-synuclein and tau. *eLife*, **7**, e36768.
24. Fong, K.W., Zhao, J.C., Song, B., Zheng, B. and Yu, J. (2018) TRIM28 protects TRIM24 from SPOP-mediated degradation and promotes prostate cancer progression. *Nat. Commun.*, **9**, 5007.
25. Su, C., Li, H. and Gao, W. (2018) TRIM28 is overexpressed in glioma and associated with tumor progression. *OncoTargets Ther.*, **11**, 6447–6458.
26. Peng, Y., Zhang, M., Jiang, Z. and Jiang, Y. (2019) TRIM28 activates autophagy and promotes cell proliferation in glioblastoma. *OncoTargets Ther.*, **12**, 397–404.
27. Addison, J.B., Koontz, C., Fugett, J.H., Creighton, C.J., Chen, D., Farrugia, M.K., Padon, R.R., Voronkova, M.A., McLaughlin, S.L., Livengood, R.H. et al. (2015) KAP1 promotes proliferation and metastatic progression of breast cancer cells. *Cancer Res.*, **75**, 344–355.
28. Diets, I.J., Hoyer, J., Ekici, A.B., Popp, B., Hoogerbrugge, N., van Reijmersdal, S.V., Bhaskaran, R., Hadjihannas, M., Vasileiou, G., Thiel, C.T. et al. (2019) TRIM28 haploinsufficiency predisposes to Wilms tumor. *Int. J. Cancer*, **145**, 941–951.
29. Halliday, B.J., Fukuzawa, R., Markie, D.M., Grundy, R.G., Ludgate, J.L., Black, M.A., Skeen, J.E., Weeks, R.J., Catchpole, D.R., Roberts, A.G.K. et al. (2018) Germline mutations and somatic inactivation of TRIM28 in Wilms tumour. *PLoS Genet.*, **14**, e1007399.
30. Hu, C., Zhang, S., Gao, X., Xu, X., Lv, Y., Zhang, Y., Zhu, Z., Zhang, C., Li, Q. et al. (2012) Roles of Kruppel-associated box (KRAB)-associated co-repressor KAP1 Ser-473 phosphorylation in DNA damage response. *J. Biol. Chem.*, **287**, 18937–18952.
31. Jin, X., Pan, Y., Wang, L., Zhang, H., Ravichandran, R., Potts, P.R., Jiang, J., Wu, H. and Huang, H. (2017) MAGE-TRIM28 complex promotes the Warburg effect and hepatocellular carcinoma progression by targeting FBPI for degradation. *Oncogenesis*, **6**, e312.
32. Tanaka, S., Pflieger, C., Lai, J.F., Roan, F., Sun, S.C. and Ziegler, S.F. (2018) KAP1 regulates regulatory T cell function and proliferation in both Foxp3-dependent and -independent manners. *Cell Rep.*, **23**, 796–807.
33. Li, J., Xi, Y., Li, W., McCarthy, R.L., Stratton, S.A., Zou, W., Li, W., Dent, S.Y., Jain, A.K. and Barton, M.C. (2017) TRIM28 interacts with EZH2 and SWI/SNF to activate genes that promote mammosphere formation. *Oncogene*, **36**, 2991–3001.
34. Wang, C., Ivanov, A., Chen, L., Fredericks, W.J., Seto, E., Rauscher, F.J. 3rd and Chen, J. (2005) MDM2 interaction with nuclear corepressor KAP1 contributes to p53 inactivation. *EMBO J.*, **24**, 3279–3290.
35. Okamoto, K., Kitabayashi, I. and Taya, Y. (2006) KAP1 dictates p53 response induced by chemotherapeutic agents via Mdm2 interaction. *Biochem. Biophys. Res. Commun.*, **351**, 216–222.
36. Allton, K., Jain, A.K., Herz, H.M., Tsai, W.W., Jung, S.Y., Qin, J., Bergmann, A., Johnson, R.L. and Barton, M.C. (2009) Trim24 targets endogenous p53 for degradation. *Proc. Natl Acad. Sci. U.S.A.*, **106**, 11612–11616.
37. Jain, A.K., Allton, K., Duncan, A.D. and Barton, M.C. (2014) TRIM24 is a p53-induced E3-ubiquitin ligase that undergoes ATM-mediated phosphorylation and autodegradation during DNA damage. *Mol. Cell. Biol.*, **34**, 2695–2709.
38. Doyle, J.M., Gao, J., Wang, J., Yang, M. and Potts, P.R. (2010) MAGE-RING protein complexes comprise a family of E3 ubiquitin ligases. *Mol. Cell. Biol.*, **30**, 963–974.
39. Bhatia, N., Xiao, T.Z., Rosenthal, K.A., Siddiqui, I.A., Thiagarajan, S., Smart, B., Meng, Q., Zuleger, C.L., Mukhtar, H., Kenney, S.C. et al. (2013) MAGE-C2 promotes growth and tumorigenicity of melanoma cells, phosphorylation of KAP1, and DNA damage repair. *J. Invest. Dermatol.*, **133**, 759–767.
40. Song, X., Guo, C., Zheng, Y., Wang, Y., Jin, Z. and Yin, Y. (2018) Post-transcriptional regulation of cancer/testis antigen MAGEC2 expression by TRIM28 in tumor cells. *BMC Cancer*, **18**, 971.
41. Patel, A., Yang, P., Tinkham, M., Pradhan, M., Sun, M.A., Wang, Y., Hoang, D., Wolf, G., Horton, J.R., Zhang, X. et al. (2018) DNA conformation induces adaptable binding by tandem zinc finger proteins. *Cell*, **173**, 221–233.
42. Ouellet, V., Zietarska, M., Portelance, L., Lafontaine, J., Madore, J., Puiffe, M.L., Arcand, S.L., Shen, Z., Hebert, J., Tonin, P.N. et al. (2008) Characterization of three new serous epithelial ovarian cancer cell lines. *BMC Cancer*, **8**, 152.
43. Zhao, Q., Wang, C., Zhu, J., Wang, L., Dong, S., Zhang, G. and Tian, J. (2011) RNAi-mediated knockdown of cyclooxygenase2 inhibits the growth, invasion and migration of SaOS2 human osteosarcoma cells: a case control study. *J. Exp. Clin. Cancer Res.*, **30**, 26.
44. Stanisavljevic, J., Porta-de-la-Riva, M., Batlle, R., de Herreros, A.G. and Baulida, J. (2011) The p65 subunit of NF-kappaB and PARP1 assist Snail1 in activating fibronectin transcription. *J. Cell Sci.*, **124**, 4161–4171.
45. Kumar, J., Fraser, F.W., Riley, C., Ahmed, N., McCulloch, D.R. and Ward, A.C. (2014) Granulocyte colony-stimulating factor receptor signalling via Janus kinase 2/signal transducer and activator of transcription 3 in ovarian cancer. *Br. J. Cancer*, **110**, 133–145.
46. Some, D., Amartely, H., Tsadok, A. and Lebendiker, M. (2019) Characterization of proteins by size-exclusion chromatography coupled to multi-angle light scattering (SEC-MALS). *J. Vis. Exp.*, **148**, e59615.

47. Kikhney, A.G. and Svergun, D.I. (2015) A practical guide to small angle X-ray scattering (SAXS) of flexible and intrinsically disordered proteins. *FEBS Lett.*, **589**, 2570–2577.
48. Peng, H., Gibson, L.C., Capili, A.D., Borden, K.L., Osborne, M.J., Harper, S.L., Speicher, D.W., Zhao, K., Marmorstein, R., Rock, T.A. *et al.* (2007) The structurally disordered KRAB repression domain is incorporated into a protease resistant core upon binding to KAP-1-RBCC domain. *J. Mol. Biol.*, **370**, 269–289.
49. Fonti, G., Marcaida, M.J., Bryan, L.C., Trager, S., Kalantzi, A.S., Helleboid, P.J., Demurtas, D., Tully, M.D., Grudin, S., Trono, D. *et al.* (2019) KAP1 is an antiparallel dimer with a functional asymmetry. *Life Sci. Alliance*, **2**, e201900349.
50. Garcia-Garcia, M.J., Shibata, M. and Anderson, K.V. (2008) Chato, a KRAB zinc-finger protein, regulates convergent extension in the mouse embryo. *Development*, **135**, 3053–3062.
51. Shibata, M. and Garcia-Garcia, M.J. (2011) The mouse KRAB zinc-finger protein CHATO is required in embryonic-derived tissues to control yolk sac and placenta morphogenesis. *Dev. Biol.*, **349**, 331–341.
52. Perlman, H., Zhang, X., Chen, M.W., Walsh, K. and Buttyan, R. (1999) An elevated bax/bcl-2 ratio corresponds with the onset of prostate epithelial cell apoptosis. *Cell Death Differ.*, **6**, 48–54.
53. Raisova, M., Hossini, A.M., Eberle, J., Riebeling, C., Wieder, T., Sturm, I., Daniel, P.T., Orfanos, C.E. and Geilen, C.C. (2001) The Bax/Bcl-2 ratio determines the susceptibility of human melanoma cells to CD95/Fas-mediated apoptosis. *J. Invest. Dermatol.*, **117**, 333–340.
54. Grote, T., Siwak, D.R., Fritsche, H.A., Joy, C., Mills, G.B., Simeone, D., Whitcomb, D.C. and Logsdon, C.D. (2008) Validation of reverse phase protein array for practical screening of potential biomarkers in serum and plasma: accurate detection of CA19-9 levels in pancreatic cancer. *Proteomics*, **8**, 3051–3060.
55. Wiles, E.T. and Selker, E.U. (2017) H3K27 methylation: a promiscuous repressive chromatin mark. *Curr. Opin. Genet. Dev.*, **43**, 31–37.
56. Appikonda, S., Thakkar, K.N. and Barton, M.C. (2016) Regulation of gene expression in human cancers by TRIM24. *Drug Discov. Today Technol.*, **19**, 57–63.
57. Herquel, B., Ouararhni, K., Khetchoumian, K., Ignat, M., Teletin, M., Mark, M., Bechade, G., Van Dorsselaer, A., Sanglier-Cianferani, S., Hamiche, A. *et al.* (2011) Transcription cofactors TRIM24, TRIM28, and TRIM33 associate to form regulatory complexes that suppress murine hepatocellular carcinoma. *Proc. Natl Acad. Sci. U.S.A.*, **108**, 8212–8217.
58. Gechijian, L.N., Buckley, D.L., Lawlor, M.A., Reyes, J.M., Paulk, J., Ott, C.J., Winter, G.E., Erb, M.A., Scott, T.G., Xu, M. *et al.* (2018) Functional TRIM24 degrader via conjugation of ineffectual bromodomain and VHL ligands. *Nat. Chem. Biol.*, **14**, 405–412.
59. Tomczak, K., Czerwinska, P. and Wiznerowicz, M. (2015) The Cancer Genome Atlas (TCGA): an immeasurable source of knowledge. *Contemp. Oncol. (Pozn)*, **19**, A68–A77.
60. Richart, L. and Margueron, R. (2020) Drugging histone methyltransferases in cancer. *Curr. Opin. Chem. Biol.*, **56**, 51–62.
61. Konze, K.D., Ma, A., Li, F., Barsyte-Lovejoy, D., Parton, T., Macnevin, C.J., Liu, F., Gao, C., Huang, X.P., Kuznetsova, E. *et al.* (2013) An orally bioavailable chemical probe of the lysine methyltransferases EZH2 and EZH1. *ACS Chem. Biol.*, **8**, 1324–1334.
62. Curry, E., Green, I., Chapman-Rothe, N., Shamsaei, E., Kandil, S., Cherblanc, F.L., Payne, L., Bell, E., Ganesh, T., Srimongkolpithak, N. *et al.* (2015) Dual EZH2 and EHMT2 histone methyltransferase inhibition increases biological efficacy in breast cancer cells. *Clin. Epigenetics*, **7**, 84.
63. Gonzalez, M.E., Li, X., Toy, K., DuPrie, M., Ventura, A.C., Banerjee, M., Ljungman, M., Merajver, S.D. and Kleer, C.G. (2009) Downregulation of EZH2 decreases growth of estrogen receptor-negative invasive breast carcinoma and requires BRCA1. *Oncogene*, **28**, 843–853.
64. Ma, A., Stratikopoulos, E., Park, K.S., Wei, J., Martin, T.C., Yang, X., Schwarz, M., Leshchenko, V., Rialdi, A., Dale, B. *et al.* (2020) Discovery of a first-in-class EZH2 selective degrader. *Nat. Chem. Biol.*, **16**, 214–222.
65. Morin, R.D., Johnson, N.A., Severson, T.M., Mungall, A.J., An, J., Goya, R., Paul, J.E., Boyle, M., Woolcock, B.W., Kuchenbauer, F. *et al.* (2010) Somatic mutations altering EZH2 (Tyr641) in follicular and diffuse large B-cell lymphomas of germinal-center origin. *Nat. Genet.*, **42**, 181–185.
66. Ennishi, D., Takata, K., Beguelin, W., Duns, G., Mottok, A., Farinha, P., Bashashati, A., Saberi, S., Boyle, M., Meissner, B. *et al.* (2019) Molecular and genetic characterization of MHC deficiency identifies EZH2 as therapeutic target for enhancing immune recognition. *Cancer Discov.*, **9**, 546–563.
67. Stevens, R.V., Esposito, D. and Rittinger, K. (2019) Characterisation of class VI TRIM RING domains: linking RING activity to C-terminal domain identity. *Life Sci. Alliance*, **2**, e201900295.
68. Pineda, C.T. and Potts, P.R. (2015) Oncogenic MAGEA–TRIM28 ubiquitin ligase downregulates autophagy by ubiquitinating and degrading AMPK in cancer. *Autophagy*, **11**, 844–846.
69. Pineda, C.T., Ramanathan, S., Fon Tacer, K., Weon, J.L., Potts, M.B., Ou, Y.H., White, M.A. and Potts, P.R. (2015) Degradation of AMPK by a cancer-specific ubiquitin ligase. *Cell*, **160**, 715–728.
70. Ivanov, A.V., Peng, H., Yurchenko, V., Yap, K.L., Negorev, D.G., Schultz, D.C., Psulkowski, E., Fredericks, W.J., White, D.E., Maul, G.G. *et al.* (2007) PHD domain-mediated E3 ligase activity directs intramolecular sumoylation of an adjacent bromodomain required for gene silencing. *Mol. Cell*, **28**, 823–837.
71. Mascle, X.H., Germain-Desprez, D., Huynh, P., Estephan, P. and Aubry, M. (2007) Sumoylation of the transcriptional intermediary factor 1beta (TIF1beta), the co-repressor of the KRAB multifinger proteins, is required for its transcriptional activity and is modulated by the KRAB domain. *J. Biol. Chem.*, **282**, 10190–10202.
72. Niazi, S., Purohit, M. and Niazi, J.H. (2018) Role of p53 circuitry in tumorigenesis: a brief review. *Eur. J. Med. Chem.*, **158**, 7–24.
73. Napoli, M. and Flores, E.R. (2020) The p53 family reaches the final frontier: the variegated regulation of the dark matter of the genome by the p53 family in cancer. *RNA Biol.*, doi:10.1080/15476286.2019.1710054.
74. Levine, A.J. (2020) p53 and the immune response: 40 years of exploration—a plan for the future. *Int. J. Mol. Sci.*, **21**, 541.
75. Jain, A.K. and Barton, M.C. (2018) p53: emerging roles in stem cells, development and beyond. *Development*, **145**, dev158360.
76. Fischer, M. (2017) Census and evaluation of p53 target genes. *Oncogene*, **36**, 3943–3956.
77. Khurana, A. and Shafer, D.A. (2019) MDM2 antagonists as a novel treatment option for acute myeloid leukemia: perspectives on the therapeutic potential of idasanutlin (RG7388). *OncoTargets Ther.*, **12**, 2903–2910.
78. Nakamura, M., Obata, T., Daikoku, T. and Fujiwara, H. (2019) The association and significance of p53 in gynecologic cancers: the potential of targeted therapy. *Int. J. Mol. Sci.*, **20**, 5482.
79. Reis, B., Jukofsky, L., Chen, G., Martinelli, G., Zhong, H., So, W.V., Dickinson, M.J., Drummond, M., Assouline, S., Hashemyan, M. *et al.* (2016) Acute myeloid leukemia patients' clinical response to idasanutlin (RG7388) is associated with pre-treatment MDM2 protein expression in leukemic blasts. *Haematologica*, **101**, e185–e188.